QUANTITATIVE SECTION SCANNING USING ORTHOGONAL TANGENT CORRECTION

David E. Kuhl, Roy Q. Edwards, Anthony R. Ricci, and Martin Reivich

Hospital of the University of Pennsylvania, Philadelphia, Pennsylvania

Orthogonal tangent correction (OTC) is introduced as an improvement of the processing technique for transverse section imaging. The initial step in this processing technique is to take an orthogonal pair of tangent data lines and form a matrix distribution that reflects the proportionality that exists between them. The matrix data are then redistributed to conform to the proportionality of each succeeding orthogonal pair of tangent lines without destroying the compatibility achieved in previous steps. The final section matrix is a high contrast image of the cross-section, the matrix distribution is compatible with all tangent values, and there is a linear relationship between matrix counts and radioactivity in the scanned object. We have already applied Orthogonal Tangent Correction to clinical brain scanning with advantage but we regard its more important role to be as another significant step toward quantitative imaging for estimate of radioactivity localized in three dimensions.

Section scanning is already useful for subjective evaluation in clinical imaging. Inherent in the method is the potential for quantitative estimates of radioactivity localized in three dimensions. This has yet to be exploited fully.

In transverse section scanning, radiation detectors make a sequence of tangential scans at regular angular intervals around the patient's head so as to view the selected cross section of the brain from many different directions. In our earliest work, we made section pictures by exposing film to a line of light that was moved with speed and orientation matched to the detector's line of view (*1*). Counting rate was used to control the brightness of the line of light that represented the line of view of the detectors through the entire section. Then we replaced this method with a digital summation technique (*2*). After processing, the transverse section picture was represented as a matrix of picture elements, each of which represented a simple average of counts detected over that address at a detector positioned on the nearest side (single-sector addition, SSA) or, alternatively, by a detector positioned on both sides (double-sector addition, DSA), for all tangent scans.

With SSA and DSA reliability and reproducibility improved, the method has had successful clinical use since then (*3,4*). But this approach yields low contrast data since all count information is smeared across the entire section picture. There is no linear relationship between counts in the section matrix and radioactivity in the patient. Given the final section matrix, it is not possible to reconstruct the original tangent lines of data. Subsequent investigations by others (*5,6*) have been directed to these same problems.

Now we introduce orthogonal tangent correction (OTC) as an improvement of our method. The initial step in this processing technique is to take an orthogonal pair of tangent data lines and form a matrix distribution that reflects the proportionality that exists between them. The matrix data are then redistributed to conform to the proportionality of each succeeding orthogonal pair of tangent lines without destroying the compatibility achieved in previous steps.

The final section matrix is a high contrast image of the cross section; compatibility is maintained between the matrix distribution and tangent values, and there is a linear relationship between matrix counts and radioactivity in the scanned object.

METHOD

Our previous DSA technique is described in simplified form in the following example: Figure 1 shows a matrix distribution which simulates a line-source phantom and the tangent values obtained from four angular scanning views of the phantom.

The first step in the DSA technique is to start with 0 deg or first pass and place the tangent value into

Received June 7, 1972; revision accepted Oct. 19, 1972.

For reprints contact: David E. Kuhl, Div. of Nuclear Medicine, Hospital of the University of Pennsylvania, 3400 Spruce St., Philadelphia, Pa. 19104.

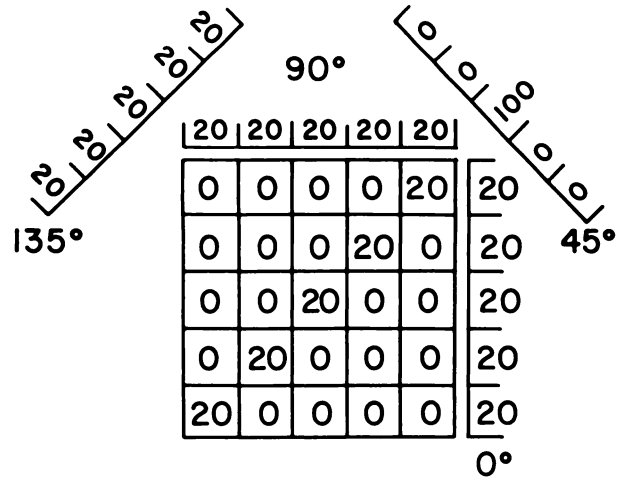

FIG. 1. Tangent values obtained from scanning simulated line-source.

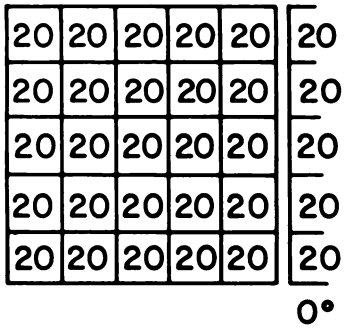

FIG. 2. DSA technique. First step places tangent values of first pass into elements in line of view.

all of the elements that are in its line of view. This is shown in Fig. 2.

The next step is to take the next line of tangent values and add them to the elements that are in their respective lines of view. This is shown in Fig. 3. This is done for each succeeding pass. Then an average is made for each cell by dividing the total in each cell by the number of scan passes. The resultant matrix is shown in Fig. 4.

Although in this simple example, the diagonal line source can be discerned, the contrast between source cells and adjacent cells is very low and does not even closely approach the original phantom values in Fig. 1. If reconstruction were exact, a transverse section scan of this matrix distribution would produce the same tangent values as those obtained from the original matrix distribution. But this is not so with DSA. The two sets of tangent values are incompatible.

The same simplified example illustrates improvement with OTC. As before, four angular scanning views of the test phantom produce the tangent values shown in Fig. 1. If one were restricted to only two views of an object, an orthogonal pair of views would give the best information concerning the internal structure of the object. Therefore, the initial step in OTC is to take an orthogonal pair of tangent lines and to form a matrix distribution that reflects the proportionality that exists between these two tangent lines.

Figure 5A shows the operating procedure for producing this orthogonal proportional distribution, and Fig. 5B shows the resulting matrix obtained from this procedure as applied to the line-source phantom in Fig. 1. It should be noted here that since the sum ΣA_N is equal to the sum ΣB_N in this simplified idealized scan situation, the result would be the same if the proportionality fraction were applied in the other direction; that is, if instead of proceeding with the $A_N/\Sigma A_N \times B_N$ operation, we were to use the other operation $B_N/\Sigma B_N \times A_N$.

In the real scanning situation, the effect of noise and attenuation will require that the tangent sums be equalized.

A closer look at Fig. 5B reveals that the resulting matrix distribution is compatible with the orthogonal tangent values; that is, a scan of this distribution represents the same tangent values as those obtained from the original phantom scan. Thus we have achieved our objective of compatibility for this pair of orthogonal tangent lines. But it is obvious that this matrix distribution does not resemble the original line source distribution.

Referring to Fig. 6A, one can see that this distribution is not compatible with the other pair of orthogonal tangent lines obtained from the original scan data. A scan of this distribution at these angles produces the tangent values shown in Fig. 6B. The problem now is to distribute the data in this matrix in such a way as to cause it to become compatible with this pair of orthogonal tangent lines without destroying the compatibility achieved in the previous step in the process. This is accomplished by forming orthogonal tangent correction factors based on the original tangent values and those obtained from this matrix distribution and applying these factors to each matrix element. This process causes an appropriate shift in the element value based on the proportional contribution of its respective orthogonal tangent values.

Using the designations shown in Fig. 7, this procedure can be illustrated by mathematical notation. For the center element, P33, the orthogonal tangent correction would be formed as follows:

In the above expression, A_3 is the original 135-deg tangent value for this element and ΣA_N is the sum of that tangent line. In this simplified phantom example, the sums of all the tangent lines will be equal and therefore drop out of this expression. In

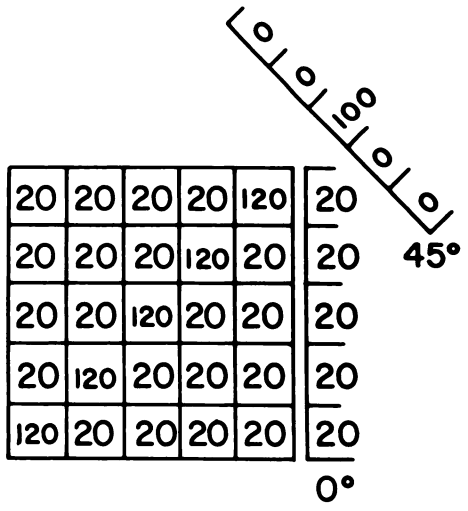

FIG. 3. DSA technique. Next step adds in tangent values of second pass to elements in line of view.

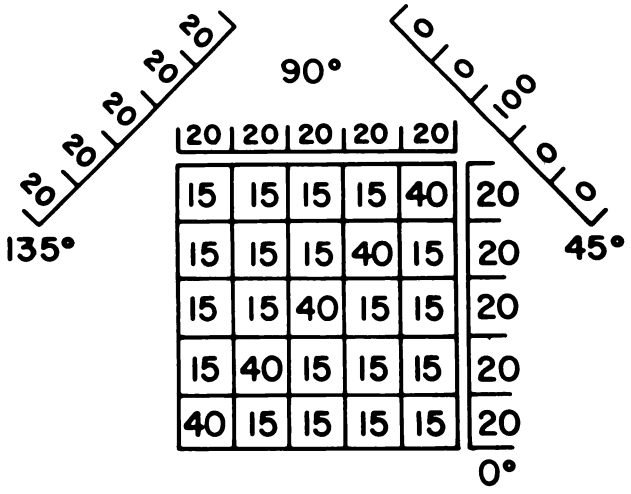

FIG. 4. DSA technique. Resultant matrix when total in each cell is average of total from all passes.

$$\frac{\frac{A_3}{\Sigma A_N}}{\frac{C_3}{\Sigma C_N}} \times \frac{\frac{B_3}{\Sigma B_N}}{\frac{D_3}{\Sigma D_N}} \times P_{33} = P_{33}\ \text{Corrected}$$

$$\frac{\frac{20}{100}}{\frac{20}{100}} \times \frac{\frac{100}{100}}{\frac{20}{100}} \times 4 = 20$$

the real scan situation, they are not equal. C_3 is the 135-deg tangent value obtained for P33 from the scan of the matrix distribution. B_3 is the original 45-deg tangent value P33, and D3 is the 45-deg tangent value for this element from the matrix scan. Forming correction factors in this manner and applying them to their respective matrix elements, we obtain the matrix distribution shown in Fig. 8. It is interesting to note here that selection of the 45-deg and 135-deg orthogonal tangent lines in the initial step, rather than the 0 deg and 90 deg pair, would have produced this first matrix in the first step. But the second step would not have shifted these data since the subsequent correction factor (0 deg and 90 deg pair) would be unity.

It is apparent from this figure that the objective of compatibility has been achieved in this example since the matrix produced is identical to the line-source phantom in Fig. 1. In addition, the use of orthogonal lines of information rather than a sequence of unidimensional information lines reduces questions of sequence sensitivity and start-stop points that have affected adversely other forms of processing we have attempted. In the real scanning situation, problems of noise, scatter, and attenuation are introduced which are not considered in this simplified discussion.

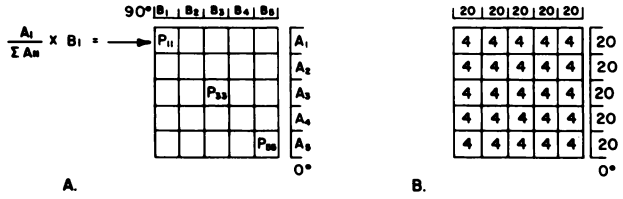

FIG. 5. OTC technique. First step. (A) Tangent values from one pass added to cells in matrix according to proportional distribution in orthogonal pass. (B) Matrix resulting from first step.

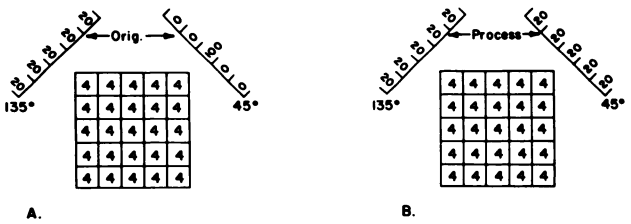

FIG. 6. OTC technique. (A) Matrix from first step is not compatible with next pair of orthogonal tangent lines of original scan data. (B) Scan of matrix resulting from first step produces a different set of tangent values.

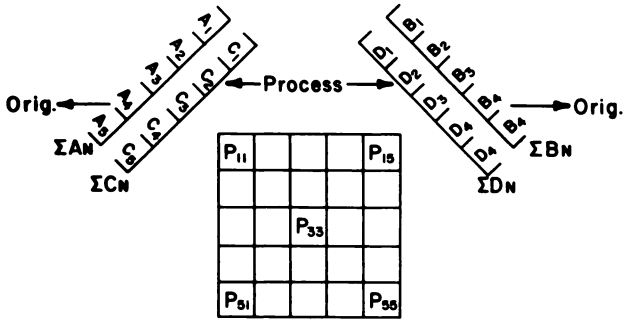

FIG. 7. OTC technique. Notation for succeeding steps. A and B are orthogonal tangent values from scanning the phantom. C and D are corresponding tangent values from scanning the processed matrix.

0	0	0	0	20
0	0	0	20	0
0	0	20	0	0
0	20	0	0	0
20	0	0	0	0

FIG. 8. OTC technique. The final matrix distribution is identical with the original distribution.

APPLICATION

In this first stage of development, the OTC process involves less than 8,000 words of computer memory and the entire operation requires less than 10 min using a Varian 620i computer (7). For data collection, tangent elements are 0.75 cm wide and the interval angle is 15 deg. Counts from opposing detectors are added. In processing there is an option for interpolation so as to produce a final picture with an increased number of smaller picture elements measuring 0.375 cm on each side. We use only tangent values corresponding to mutual orthogonal intersections within a "valid area" which is established for each scan. This area may be a disk shape to represent the scan field, or it may have the boundaries of the scanned object itself if these are known accurately.

Spatial resolution. With DSA counts from any source in the section plane are registered throughout the plane. This is not so with OTC. The undesirable degeneration of spatial resolution with DSA is demonstrated in Fig. 9. With DSA the image of sectioned line source is a star pattern extending throughout the section plane. With OTC the image is a small disk.

The importance of improved spatial resolution in clinical section scanning is demonstrated in Fig. 10. These are scans of a 40-year-old woman who was subsequently proven to have a meningioma of the left cavernous sinus with lateral extension over the left petrous bone. The tumor involves two-thirds of the floor of the middle fossa and has a medial margin at the left lateral wall of the sella. Both section pictures were made from the same original scan data taken close to the base of the brain. Note the advantage of either section over the rectilinear scan in showing the distribution of this lesion. Note that the OTC process is superior to the DSA process in demonstrating the boundaries of the tumor because the spatial resolution in the picture is much better.

Quantification. We performed an experiment to estimate how accurately the method might predict

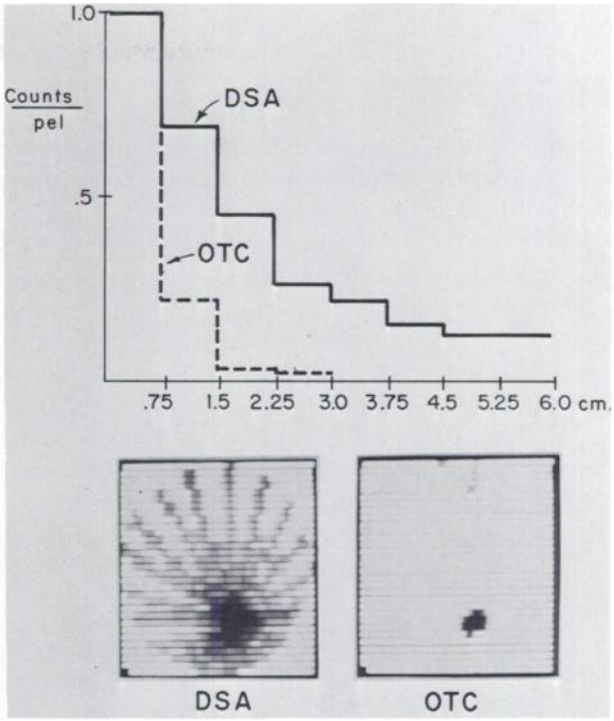

FIG. 9. Original data of a sectioned line-source processed with DSA and OTC. Spatial resolution is worse with DSA which spreads all count data across the section plane and produces large star artifact.

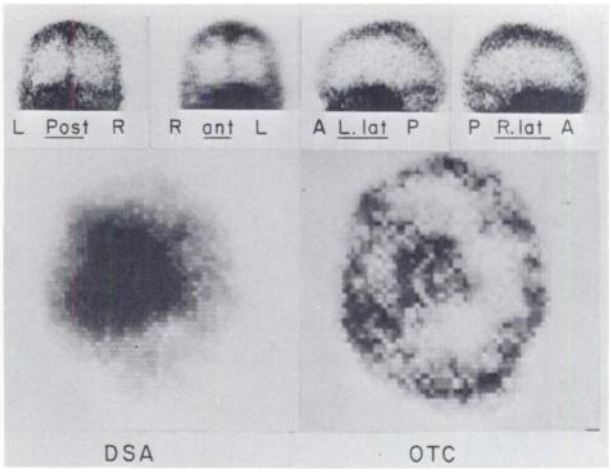

FIG. 10. Because of superior resolution and validity of data, OTC processed section demonstrates better boundaries of meningioma of left cavernous sinus which has extended over left petrous bone. Eighty-thousand counts were recorded in section scan. Rectilinear scans are shown above section pictures.

the distribution of radioactivity in a transverse section of the head. The phantom was a hexagonal (close-packed) array of 37 plastic bottles. The diameter of each bottle was 3.1 cm; the widest dimension of the array was 22 cm. Spaces between bottles were plugged with wooden pegs. Each bottle was filled with ^{99m}Tc solution that had a relative concentration of 1, 2, 3, 4, or 5 that was assigned according to a table of random numbers.

Separate transverse section scans* were made with the bottles in two different random distributions and then with the same concentration in all bottles to represent a "uniform" field distribution (UFD). After OTC processing, counts were summed within a 2 × 2-cm area corresponding to the position of each bottle in all scans.

The relative distribution of radioactivity in the section plane was expressed in terms of the true fraction (F_t) of the total radioactivity in the phantom which was present in each bottle or region of the phantom. The estimate of this was F_0, the corresponding value determined by section scan. For each bottle F_0 was calculated by taking the ratio of counts summed at that position to counts summed at a corresponding position in the UFD scan† and then normalizing so that the sum of F_0 for all bottles equalled 1. The results are shown in Fig. 11. There is a good linear correlation between the measured fractional content F_0 and the true fractional content F_t. The effect on correlation is shown for a difference in the total counts per scan and for three different choices of areas for regional summation (single bottle, three bottles, or nine bottles). As expected, correlation is best when a larger number of counts are detected and comparison is made between larger areas. But it is important to recognize in Fig. 11 that correlation is really quite good for small regions and count totals that are practical to achieve in clinical scanning.

* Mark III detector and collimator (*3*); 2 × ½ in. NaI (Tl) crystal and focused collimator. Pulse-height analyzer window was 30 keV.

† This maneuver reduces the effect of attenuation. When distribution in terms of μCi/ml is required:

$$\text{Concentration } (\mu\text{Ci/ml}) = \frac{\text{regional counts in scanned object}}{\text{regional counts/}\mu\text{Ci/ml in UFD}}$$

where the geometry of the UFD is constructed equal to that of the scanned object.

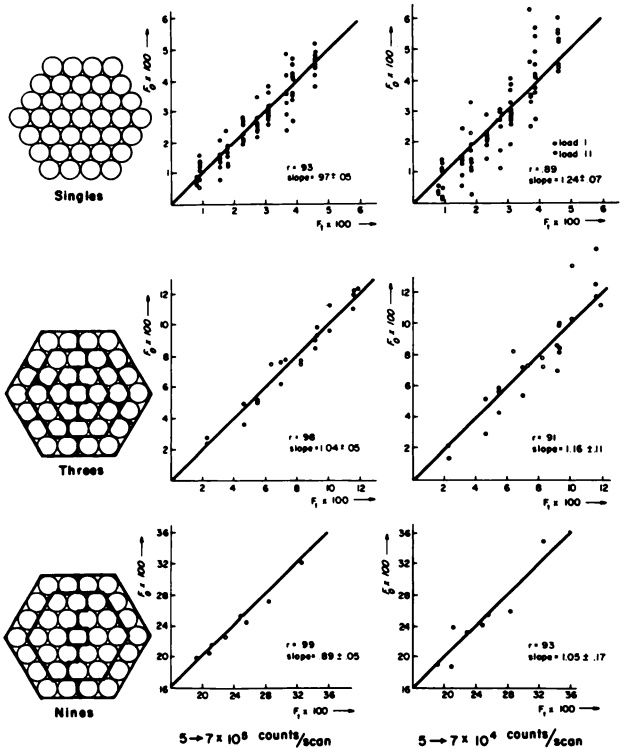

FIG. 11. Correlation of true (F_t) and estimated (F_0) fractional content of radioactivity in transverse section of 37-bottle phantom with relative concentrations distributed randomly. Data are shown for two different count totals and for three different areas of regional count summation.

CONCLUSION

Although we have applied OTC to brain tumor scanning with advantage, we regard its more important role to be as another significant step toward quantitative imaging for estimate of radioactivity localized in three dimensions. Using very simple attenuation correction, the section matrix with OTC provides an unbiased estimate of radionuclide concentration within the section plane which was never possible with the DSA method. Further work is required to define more accurately the limits of precision and accuracy possible with this approach. The successful application of the method might then open the way to quantitative tomographic scanning as a means of assessing the function of small structures deep within the body, which is not now easily accomplished.

ACKNOWLEDGMENT

We are indebted to Robert J. Yacob and Nelson L. Marin for technical assistance. This project was supported by USAEC Contract AT(30-1)-3175, USPHS Research Grant CA-04456, USPHS Research Grant NS 06314-07, and USPHS Career Research Development Award 5 K03 HE 11896-07 (Dr. Reivich). NYO-3175-70.

REFERENCES

1. KUHL DE, EDWARDS RQ: Image separation radioisotope scanning. *Radiology* 80: 653–662, 1963

2. KUHL DE, EDWARDS RQ: Reorganizing data from transverse section scans using digital processing. *Radiology* 91: 975–983, 1968

3. KUHL DE, EDWARDS RQ: The Mark III scanner: a compact device for multiple-view and section scanning of the brain. *Radiology* 96: 563–570, 1970

4. KUHL DE, SANDERS TP: Characterizing brain lesions using transverse section scanning. *Radiology* 98: 317–328, 1971

5. MUEHLLEHNER G, WETZEL RA: Section imaging by computer calculation. *J Nucl Med* 12: 76–84, 1971

6. CHESLER DA: Three-dimensional activity distribution from multiple position scintigraphs. *J Nucl Med* 12: 347–348, 1971

7. KUHL DE, EDWARDS RQ: A hybrid processor for modifying and rearranging radionuclide scan data under direct observation. *Radiology* 92: 558–570, 1969